



3 4456 0549301 6

CENTRAL RESEARCH LIBRARY
DOCUMENT COLLECTION**OAK RIDGE NATIONAL LABORATORY**

operated by

UNION CARBIDE CORPORATION

for the

U. S. ATOMIC ENERGY COMMISSION



ORNL - TM - 1220

COPY NO. - 63

DATE - August 19, 1965

MULTIPLICATION FACTOR OF URANIUM METAL BY ONE-VELOCITY
MONTE CARLO CALCULATIONS*

J. T. Mihalezo

Abstract

A method is described for predicting the neutron multiplication factors of geometrically complicated configurations of unreflected unmoderated enriched-uranium metal from the results of two delayed-critical experiments in simple geometry, one with a nearly minimum surface-to-volume ratio and the other with a large surface-to-volume ratio. The method requires two constants characteristic of the metal. These are the total collision cross section (Σ_t) and the number of neutrons produced per collision ($\nu\Sigma_f/\Sigma_t$), which are obtained from the two experiments by using S_{12} transport theory calculations with isotropic scattering. These factors, together with the assumption of isotropic scattering, are then used in OSR Monte Carlo neutron transport calculations to predict the multiplication factors. The method has been tested by predicting the multiplication factors of 21 different delayed-critical configurations to within a standard deviation of 1.5%.

*Submitted for publication in Nuclear Science and Engineering with Appendices deleted.

NOTICE

This document contains information of a preliminary nature and was prepared primarily for internal use at the Oak Ridge National Laboratory. It is subject to revision or correction and therefore does not represent a final report. ~~The information is not to be abstracted, reprinted or otherwise given public dissemination without the approval of the ORNL patent branch, Legal and Information Control Department.~~

CENTRAL RESEARCH LIBRARY
DOCUMENT COLLECTION**LIBRARY LOAN COPY**

DO NOT TRANSFER TO ANOTHER PERSON

If you wish someone else to see this document, send in name with document and the library will arrange a loan.

LEGAL NOTICE

This report was prepared as an account of Government sponsored work. Neither the United States, nor the Commission, nor any person acting on behalf of the Commission:

- A. Makes any warranty or representation, expressed or implied, with respect to the accuracy, completeness, or usefulness of the information contained in this report, or that the use of any information, apparatus, method, or process disclosed in this report may not infringe privately owned rights; or
- B. Assumes any liabilities with respect to the use of, or for damages resulting from the use of any information, apparatus, method, or process disclosed in this report.

As used in the above, "person acting on behalf of the Commission" includes any employee or contractor of the Commission, or employee of such contractor, to the extent that such employee or contractor of the Commission, or employee of such contractor prepares, disseminates, or provides access to, any information pursuant to his employment or contract with the Commission, or his employment with such contractor.

Introduction

A wide variety of unmoderated and unreflected critical experiments with geometrically complicated configurations of 93.2% ^{235}U -enriched uranium metal ($\rho = 18.7\text{g/cm}^3$) have been reported.¹⁻⁵ Some of these experiments have been analyzed by a many-velocity Monte Carlo method which provides as detailed a treatment of the neutron energy as the cross-section information will allow.⁶ This paper shows that if only the multiplication factors of unreflected homogeneous assemblies such as these are desired, a simpler Monte Carlo treatment of monoenergetic neutrons is adequate. This "one-velocity" method, summarized in Reference 7, has two advantages over the more detailed one: (1) only two input constants characteristic of the material are required and (2) the necessary computer time is reduced by a factor of four to five. It has the disadvantage, of course, that the only meaningful result that can be obtained is the multiplication factor.

The method has been tested by calculating the multiplication factors for 21 uranium-metal assemblies that had been made critical experimentally. They included spheres, cylinders, parallelepipeds, and cylindrical annuli, both separately and in certain combinations; arrays of cylinders in lattices; and one combination of cylinders, parallelepipeds, and a hemisphere.

Method of Obtaining One-Velocity Constants

The constants required as input for the Monte Carlo calculations are the collision cross section, Σ_t , and the number of neutrons produced per collision, $\nu\Sigma_f/\Sigma_t$, which satisfy the one-velocity Boltzmann transport

OAK RIDGE NATIONAL LABORATORY LIBRARIES



3 4456 0549301 6

equation for two experiments in simple geometry. One experiment should have a nearly minimum surface-to-volume ratio and the other a large surface-to-volume ratio. Although it is preferable that these be delayed-critical experiments, since then k_{eff} can be measured more accurately and the proper neutron spectrum exists, the data from two subcritical experiments will also give the required constants provided k_{eff} is known and the spectrum is the same as that in a critical system. The solution of the transport equation yields Σ_t as a function of $\nu\Sigma_f/\Sigma_t$ for each geometry, and the values of Σ_t and $\nu\Sigma_f/\Sigma_t$ common to both geometries are characteristic of the material.

The experiments used to determine the constants for the calculations reported here were 17.770-cm- and 38.087-cm-diam cylinders whose dimensions are given in Table I. Since the Boltzmann transport equation cannot be solved exactly in cylindrical geometry, the values of $\nu\Sigma_f$ and Σ_t for the two cylinders were obtained from S_{12} transport theory calculations using the DDK code⁸ with a 16 x 16 grid of space points describing the geometries and a convergence criteria, ϵ , of 10^{-4} . The results of the calculations are given in Table II. The actual experimental geometries were slightly under delayed critical, so the values of $\nu\Sigma_f$ obtained from the calculations [which iterates $\nu\Sigma_f$ until the multiplication constant is unity and evaluates $\Delta(\nu\Sigma_f)/\Delta k$] were corrected to those observed experimentally. These corrected values of $\nu\Sigma_f$ are also given in Table II. Figure 1 shows the corrected values of $\nu\Sigma_f/\Sigma_t$ vs Σ_t for the two cylinders from which the values of Σ_t and $\nu\Sigma_f/\Sigma_t$ common to both cylinders are found to be 0.2385 cm^{-1} and 0.371, respectively. One-velocity S_{12} calculations were also performed for a cylindrical uranium-metal annulus with outside and inside

Table I. Measured Dimensions of Uranium-Metal Assemblies

Assembly	Diameter (cm)	Height of Radial Increments of ^a					Average Uranium Density (g/cm ³)	Multi- plication Factor ^b
		0-8.89 cm	8.89-11.43 cm	11.43-13.97 cm	13.97-16.51 cm	16.51-19.05 cm		
Cylinder 1	17.770	12.626	-	-	-	-	18.759	0.9998
Cylinder 2	38.087	7.635	7.790	7.795	7.640	7.630	18.705	0.9986
Annulus	38.090 OD 22.865 ID	-	-	14.938	15.131	15.141	18.705	0.9982

a. The units available for the construction of the assemblies included 8.89-cm-diam cylinders and 2.54-cm-wide cylindrical annuli having inside radii of 8.89, 11.43, 13.97, and 16.51 cm, all in a variety of thicknesses. The over-all height of the assembled units varied slightly from section to section.

b. Based on $\beta_{\text{eff}} = 0.0068$.

Table II. Σ_t and $\nu\Sigma_f$ from One-Velocity S_{12} Calculations^a
for Cylinders and Annuli

Σ_t (cm^{-1})	$\nu\Sigma_f$ (cm^{-1}) ^b			Corrected ^c $\nu\Sigma_f$ (cm^{-1})		
	17.770-cm- Diam Cylinder	38.087-cm- Diam Cylinder	Annulus	17.770-cm- Diam Cylinder	38.087-cm- Diam Cylinder	Annulus
0.050	0.128024 0.128028 ^d	0.114513	0.117892	0.128002	0.114354	0.117681
0.100	0.115082	0.106532	0.108446	0.115061	0.106382	0.108419
0.150	0.104165	0.099472	0.100530	0.104146	0.099334	0.100351
0.200	0.094882 0.094894 ^d	0.093168	0.093754	0.094873	0.093042	0.093586
0.225	0.090779	0.090272	0.090734	0.090762	0.090140	0.090571
0.250	0.086966	0.087519	0.087910	0.086950	0.087394	0.087753
0.300	0.080137 ^d 0.080126	0.024270	0.082771	0.080122	0.082314	0.082623
0.350	0.074215	0.077840	0.078225	0.074202	0.077689	0.078085
0.400	0.069016 ^d 0.069053	0.073678	0.074183	0.069034	0.073577	0.074050
0.600	0.053727	0.060487	0.061554	0.053717	0.060409	0.061447
0.800	0.043784	0.051098	0.052663	0.043775	0.051034	0.052567
1.000	0.036864	-	-	0.036858	-	-
1.200	0.031803	0.038753	0.040920	0.031797	0.038703	0.040839

a. 16 x 16 grid, $\epsilon = 10^{-4}$, DDK calculations.

b. These values are for the assemblies of Table I having $k_{\text{eff}} = 1$.

c. These values are for the assemblies of Table I having the experimentally observed values of k_{eff} . They were obtained from the values of $\nu\Sigma_f$ given in the preceding three columns, the calculated factor $\Delta(\nu\Sigma_f)/\Delta k$, and the values of β_{eff} reported in Ref. 1.

d. Values determined from S_{16} calculations.

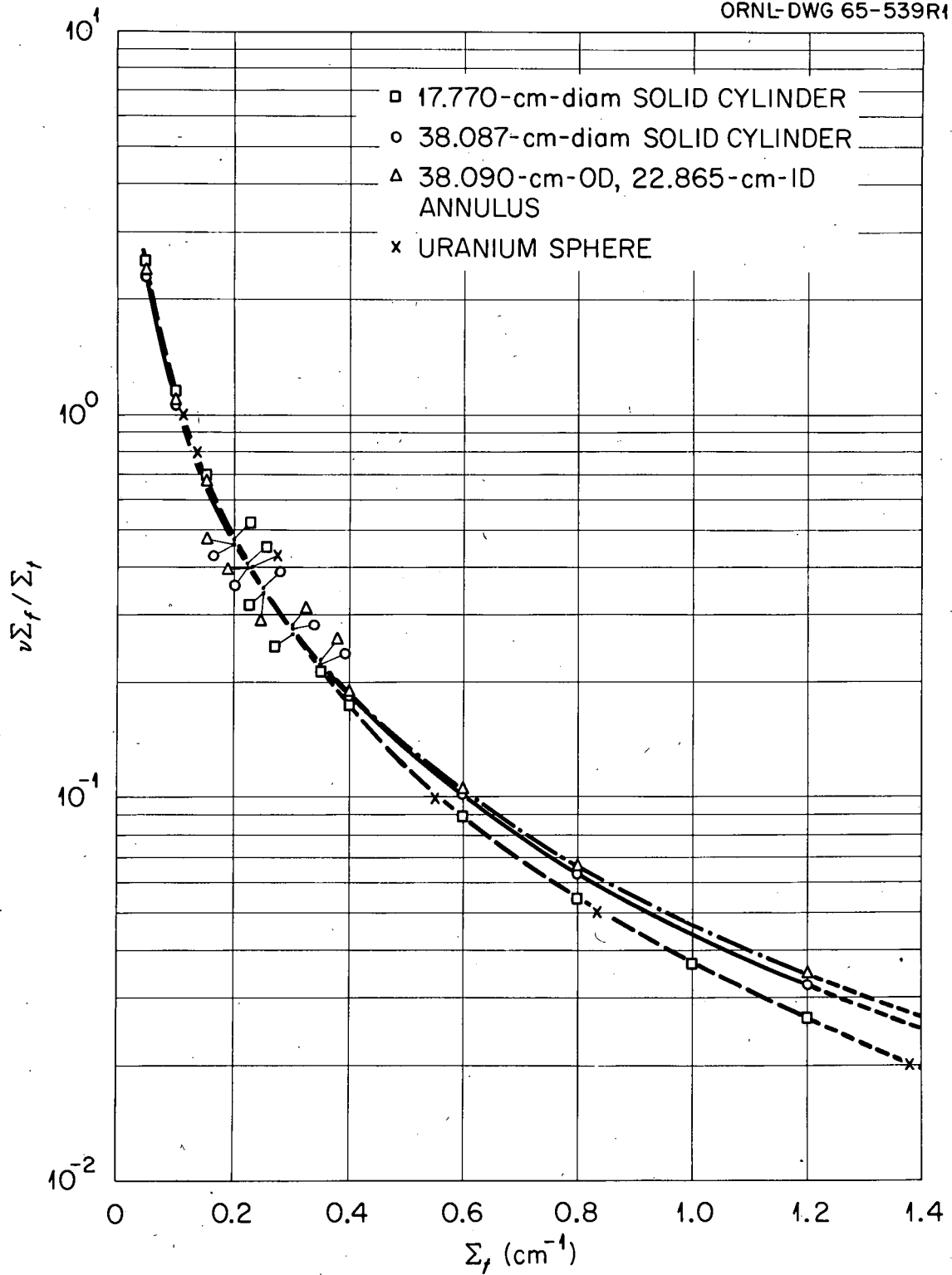


Fig. 1. Corrected Values of $\nu \Sigma_f / \Sigma_t$ vs Σ_t for Several Enriched Uranium Metal Configurations.

diameters of 38.090 and 22.865 cm, respectively. The dimensions of the annulus and the results of the calculations are also given in Tables I and II and in Fig. 1. They show that values of Σ_t and $\nu\Sigma_f/\Sigma_t$ common to the 17.78-cm-diam cylinder and the annulus, 0.2292 cm^{-1} and 0.393, are almost identical to those obtained from the two cylinders and indicate their insensitivity to the shape of the assembly.

If one of the constants is already known, the value of the other constant can be determined from a single experiment. To demonstrate this, a value of $\nu\Sigma_f/\Sigma_t = 0.4$, calculated by Carlson and Bell⁹ (see Appendix A) for a critical sphere having a radius of 1.9854 mean free paths, was used to determine Σ_t for the 8.718-cm-diam uranium-metal sphere (Godiva I) of LASL.¹ Since the ^{235}U enrichment of Godiva (93.8 wt% ^{235}U) and its uranium density (18.75 g/cm^3) are slightly different from those of the materials for which these calculations are being made (93.2% and 18.7 g/cm^3), small corrections to the constants obtained were necessary. The collision cross section was reduced by multiplying it by the ratio of the uranium densities, and the value of $\nu\Sigma_f/\Sigma_t$ was reduced by multiplying it by the ratio of the enrichments. The latter correction assumes that negligible ^{238}U fissions occur in these assemblies. The corrected values of Σ_t and $\nu\Sigma_f/\Sigma_t$ are 0.2271 cm^{-1} and 0.3974, respectively.

The results of further transport theory calculations, reported in Table III, show the multiplication factor to depend only slightly on the values of the constants within the range established by the above geometric combinations. Transport theory was used for determining the constants in preference to the Monte Carlo method because of the large statistical error, 1% for reasonable machine time, associated with the latter.

Table III. Dependence of Calculated Multiplication Factors on the One-Velocity Constants

Source of Constants	Σ_t (cm ⁻¹)	$\nu\Sigma_f/\Sigma_t$	Calculated Multiplication Factors for Critical Geometries ^a	
			17.770-cm-diam Cylinder	Annulus
Uranium Sphere	0.2271	0.3974	0.9977	0.9973
17.770- and 38.087-cm-diam Cylinders	0.2385	0.371	0.9991	0.9936
17.770-cm-diam Cylinder and Annulus	0.2292	0.393	0.9993	0.9980

a. S_{12} , $\epsilon = 10^{-4}$, 16 x 16 grid. See Table I for dimensions and experimental multiplication factors of the assemblies.

The determination of the one-velocity constants by the solution of the Boltzmann neutron transport equation for two delayed critical geometries has the advantage that knowledge of the fuel-material properties is not required. It is not necessary to go through the cumbersome tasks of averaging the cross sections (which may not be well known) for the material over a neutron energy spectrum (which also may not be well known) and of correcting for the effects of assuming isotropic scattering.

Monte Carlo Calculations of Delayed Critical Assemblies

Method. The calculations which used the constants from the S_{12} solutions were performed with the O5R Monte Carlo code¹⁰ which has a geometry routine that divides space into parallelepipeds and describes the material boundaries within the parallelepipeds by quadratic functions. Independent functions can be used within each parallelepiped. The O5R code calculates the spatial fission distribution from a batch of source neutrons put into the system on some assumed initial distribution. This resulting fission distribution is then assigned to the succeeding batch of neutrons and a new fission distribution is obtained. This process is repeated until the spatial effects of the assumed distribution disappear and the desired statistics are obtained. Since, due to statistical fluctuations in the spatial distribution of neutrons in each batch, it is difficult to determine convergence by examination of the fluctuating source distribution, the so-called matrix method is used to determine spatial convergence. If F_{ij} is the probability that a neutron born in region i produces a neutron in region j , a matrix is formed whose elements are F_{ij} . The batches with the nonconverged source distribution provide useful information for the

calculation of F_{ij} if the system is divided into a sufficient number of regions. The source distribution obtained from the first batch is iterated with this matrix until a converged source distribution is obtained. The number of iterations required for a converged source distribution is the average number of batches that need to be calculated before spatial convergence is obtained. The desired statistical accuracy of the results determines the number of additional batches needed. Since for unreflected uranium-metal assemblies the average number of collisions before leakage is about two, the initial source distribution is not important. A comparison of the effects of the assumed source distribution for a sphere is given in Appendix B.

The multiplication factor is computed by two methods: the batch method and the matrix method. The first calculates the ratio of the number of neutrons produced to the number of source neutrons in each batch and averages them over all the batches using the matrix of F_{ij} to determine when the effects of the assumed initial source distribution have disappeared. Only subsequent batches are used in computing the average batch multiplication factors. The second, or matrix, method divides the assembly into a number of regions, computes the probability that a neutron born in any region will produce a neutron in any other region, forms a matrix of these probabilities, and calculates the multiplication factor, which is the largest eigenvalue of this matrix. The multiplication factor computed by the matrix method was always within the standard deviation of that computed by the batch method.

The multiplication factor as a function of batch number for a delayed critical uranium sphere, Godiva I, is given in Fig. 2 assuming a

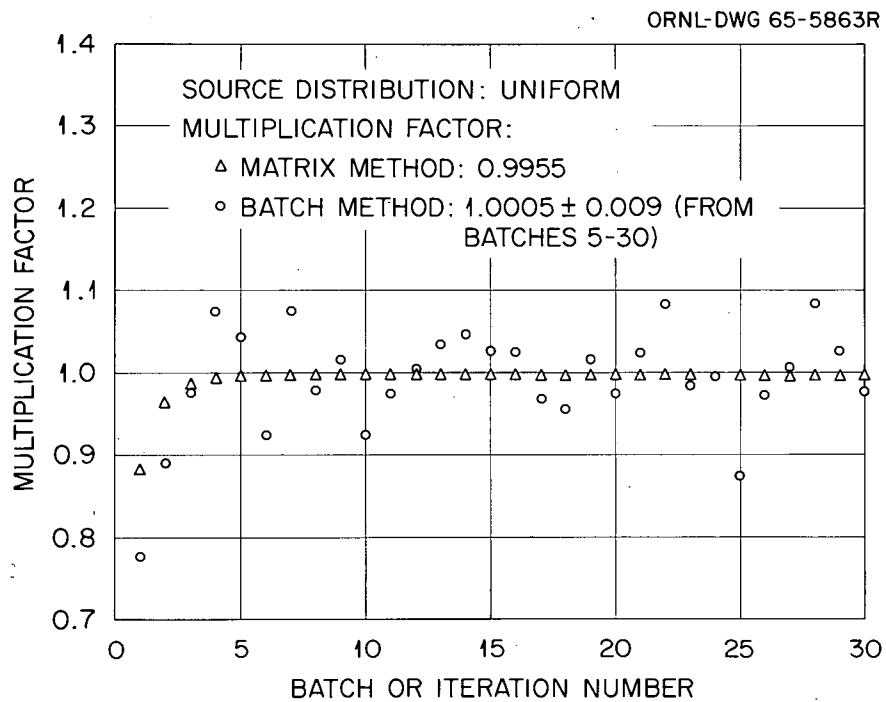


Fig. 2. Multiplication Factor vs Batch Number or Iteration Number for a Delayed Critical Uranium Sphere (Godiva I).

uniform initial distribution in space. Also plotted in this figure is the multiplication factor for the different iterations of the matrix of F_{ij} . The matrix iteration indicates that the effects of the assumed source distribution on the multiplication factor disappear after iteration five and that the source distribution converges after about seven batches.

Results. Since, as observed in Table III, the variations in the three pairs of one-velocity constants do not significantly affect the multiplication factor, the values used in the calculations of the critical experiments were $\Sigma_t = 0.2271 \text{ cm}^{-1}$ and $\nu\Sigma_f/\Sigma_t = 0.3974$. Some of the experiments calculated are illustrated in Figs. 3-5, and the others are described in Table IV. This table also gives the multiplication factor calculated by the batch method and, for most of the experiments, by the matrix method also. The values of the multiplication factors of the 21 experiments calculated by the batch method are between 0.971 to 1.028, with an average of 1.002 ± 0.014 , and with the statistical errors of individual values (standard deviations) ranging from ± 0.009 to ± 0.014 . The average of the multiplication factor for 16 experiments calculated by the matrix method is 1.001 ± 0.015 .

The differences between the calculated and experimental multiplication factors are either statistical or result from errors introduced by differences in the spectra of the various assemblies. The close agreement of the calculated and experimental values implies strongly that the differences are statistical.

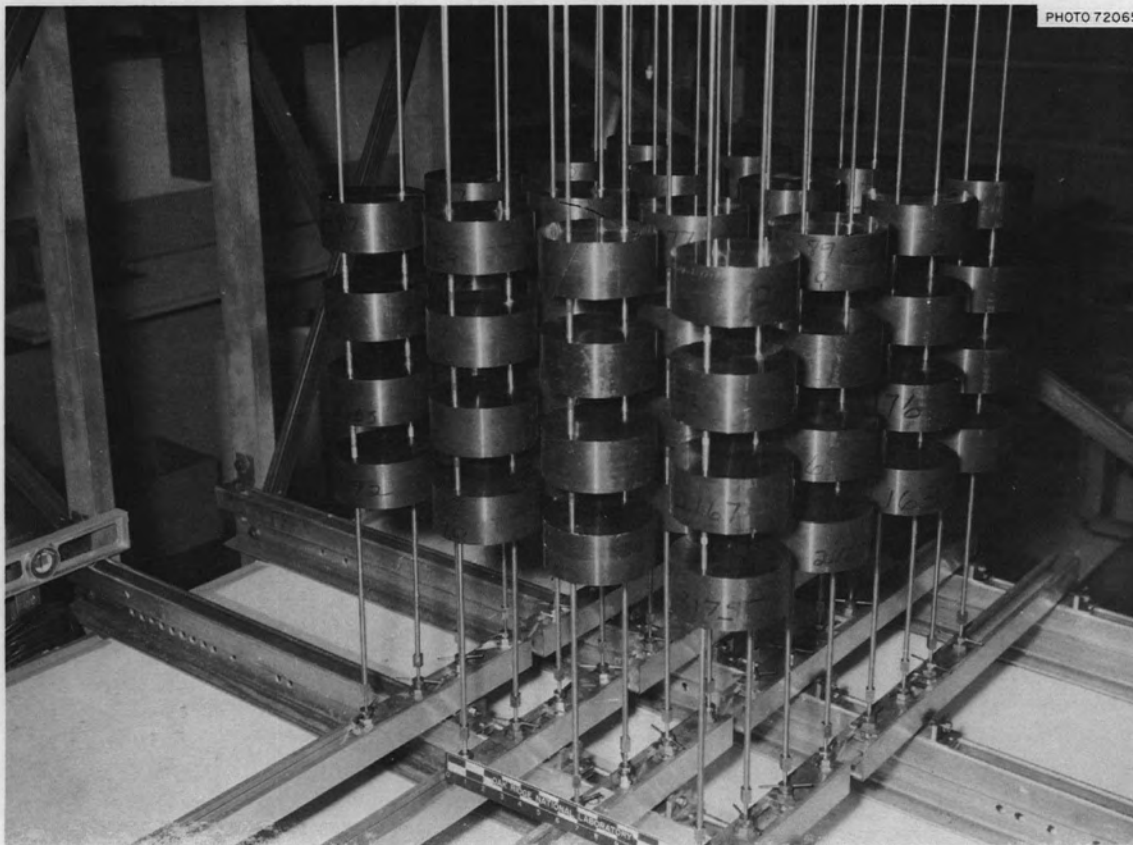


Fig. 3. Three-Dimensional Array (4 x 4 x 4) of 10.5-kg Cylinders of Uranium Metal.

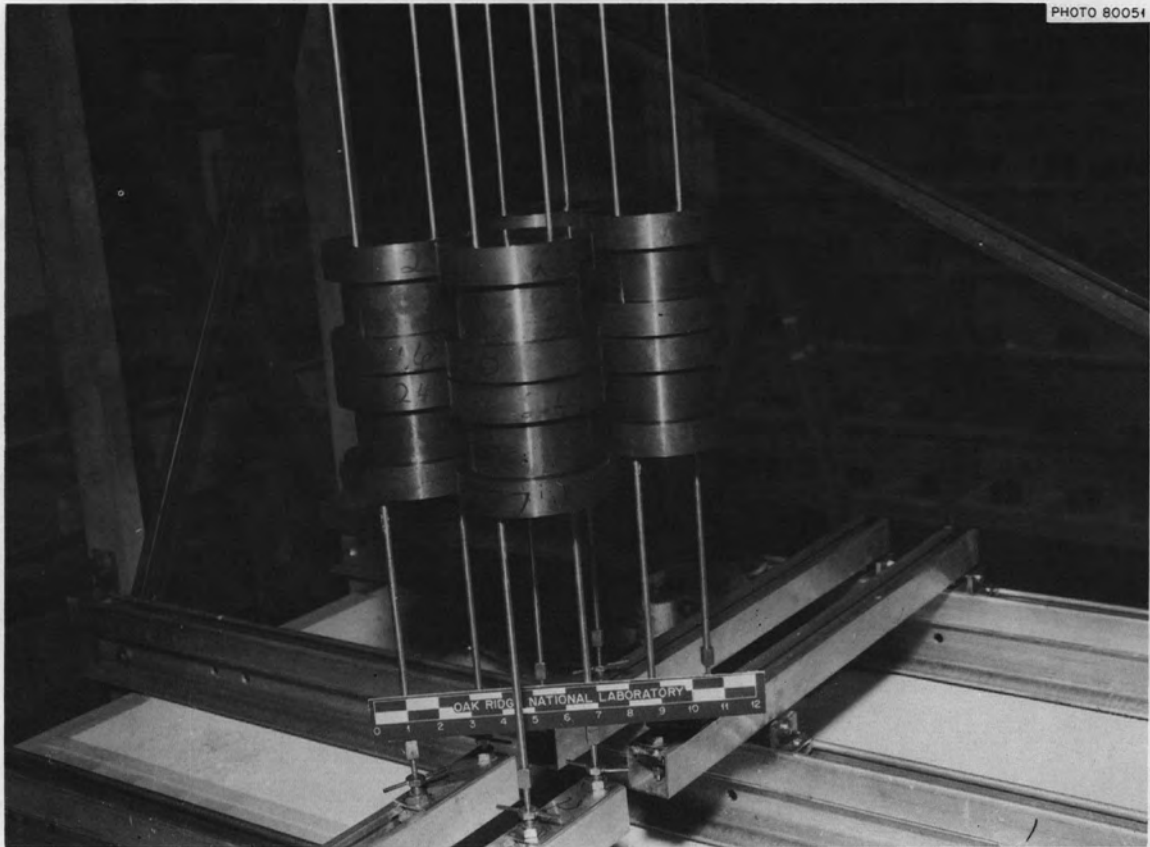


Fig. 4. Three-Dimensional Array (2 x 2 x 2) of 15.7-kg Units of Uranium Metal. Each unit consists of a 11.45-cm-diam x 5.38-cm-high cylinder between two 9.16-cm-diam x 4.32-cm-high cylinders.

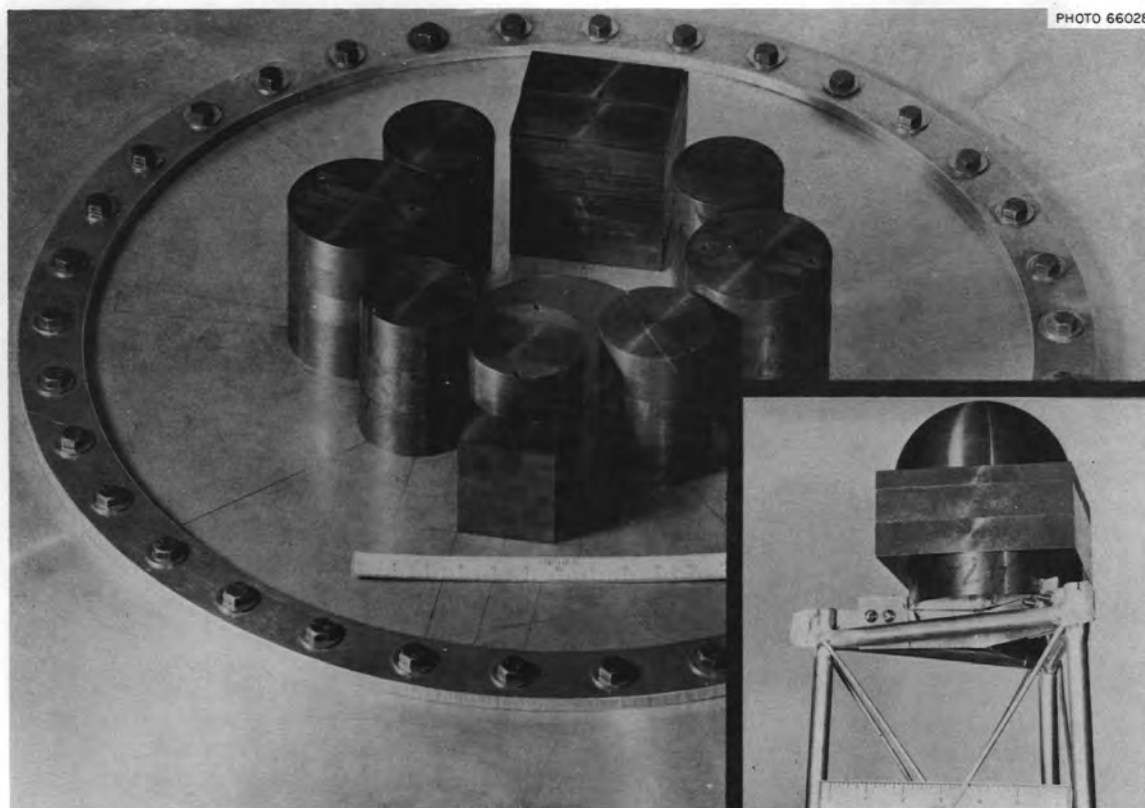


Fig. 5. Critical 93.2% ^{235}U -Enriched Uranium Metal Assembly with Eight-Unit Upper Section and an Irregularly Shaped Centerpiece (Inset). The unit at the top of the photograph is an approximate parallelepiped whose base is 5 by 5 in. and whose height varies in three steps (5.14, 5.27, and 4.39 in., front to back); the opposite unit is a parallelepiped with a 3 by 5 in. base and a 3.51-in. height topped by a 3.60-in. diam by 1.70-in. cylinder; the four small cylinders are 3.59 in. in diameter and 5.11 in. high; and the two large cylinders are 4.5 in. in diameter and 5.3 in. high. The centerpiece, which penetrated the hole in the support diaphragm, consists of a 4.5-in. diam by 1.11-in. cylinder topped by a parallelepiped with a 5.00 by 5.00 in. base and a 2.25-in. height and by a hemisphere with a 2.39-in. radius.

Table IV. One-Velocity Multiplication Factors for Uranium-Metal Geometries

Geometry	Multiplication Factor ^a	
	Batch Method ^b	Matrix Method ^b
Uranium Sphere Dimension	1.005	1.013
	1.003	0.995 ^c
	1.015	1.015 ^d
Cylinder, ^e 38.10 cm diam x 7.65 cm high	1.028	1.023
Two Coaxial Cylinders ^e		
Each 38.10 cm diam x 6.04 cm high, flat faces separated 12.27 cm	1.002	
Each 17.78 cm diam x 7.31 cm high, flat faces separated 0.86 cm	0.986	
Cylindrical annulus, ^e 38.10 cm OD, 22.86 cm ID, 14.98 cm high	1.020	1.022
	1.014 ^f	
Parallelepiped, 12.70 x 12.70 x 23.19 cm	0.996	0.994
Two Parallelepipeds ^g		
Each 20.32 x 25.40 x 7.94 cm, large faces separated 12.45 cm	1.014	1.008
Each 20.32 x 25.40 x 5.08 cm, large faces separated 0.97 cm	0.997	0.994
Cylinder and Cylindrical Annulus ^h	1.007	0.999
 Annulus: 38.1 cm OD, 27.94 cm ID Cylinder: 17.78 cm diam Each: 10.11 cm High		
Cylindrical Annulus and Parallelepiped ^h	1.011	1.010
 Annulus: 38.10 cm OD, 27.94 cm ID Parallelepiped: 12.70 cm square Each: 12.98 cm high		
Cylindrical Annulus and Two Parallelepipeds ^h	1.012	1.008
 Annulus (two sections combined): 38.10 cm OD, 27.94 cm ID, 12.98 cm high		
Upper Section		
 Parallelepipeds: 12.70 cm square No. 1, 7.62 cm high; No. 2, 11.18 cm high		
Lower Section		

Table IV. (Continued)

Geometry	Multiplication Factor ^a					
	Batch Method ^b	Matrix Method ^b				
Three-Dimensional Arrays of Cylindrical Units ⁱ						
Array	Unit Diameter (cm)	Unit Height (cm)	Surface Separation ^j (cm)	Unit Mass (kg U)		
2 x 2 x 2	11.49	8.08	0.90	15.7	0.975	0.966
	11.51	10.77	2.25	21.9	0.997	0.993
3 x 3 x 3	11.51	5.38	2.01	10.5	1.004	1.001
	11.48	10.77	6.36	20.9	0.995	0.993
4 x 4 x 4 ^k	11.51	5.38	3.95	10.5	0.971	
4 x 4 x 1	11.49	10.77	1.52	20.9	0.993	0.988
2 x 4 x 2	11.49	10.77	3.89	20.9	0.997	
2 x 2 x 2	Each unit a 11.45-cm-diam x 5.38-cm-high cylinder between two 9.16-cm-diam x 4.32-cm-high cylinders			15.7	1.010	
2 x 2 x 2 ^l	Each unit a 9.12-cm-diam x 4.32-cm-high cylinder between two 11.49-cm-diam x 2.69-cm-high cylinders			20.9	0.977	0.971
Eight units of various shapes arranged in a circle around an irregularly shaped centerpiece. ^m					1.022	1.017
					0.997 ^f	

- a. 12,000 neutron histories in 30 batches; $\Sigma_t = 0.2271 \text{ cm}^{-1}$; $\nu\Sigma_f/\Sigma_t = 0.3974$. Uniform initial neutron source distribution except where noted. The experimental values of the multiplication factors varied between 0.998 and 1.002.
- b. Statistical errors of individual values (standard deviations) vary from ± 0.009 to ± 0.014 ; the average of the batch multiplication factors for all the different geometries is 1.002 ± 0.014 ; the average of the matrix multiplication factors is 1.001 ± 0.015 . The overall average is 1.001 ± 0.015 .
- c. Point source.
- d. Cosine source.
- e. See Ref. 2.
- f. Repeat of calculation with different initial random number.
- g. See Ref. 3.
- h. See Ref. 6.
- i. See Ref. 5.
- j. Equal in three dimensions.
- k. See Fig. 3.
- l. See Fig. 4.
- m. See Fig. 5.

Conclusions

The one-velocity Monte Carlo method of calculation has been shown to yield multiplication factors which agree with the experimental values for delayed-critical unmoderated and unreflected enriched-uranium metal in complicated geometries to within a standard deviation of about 1.5%. Considering this accuracy, the method should be useful for predicting the multiplication factors of complicated configurations of unmoderated and unreflected uranium metal of any enrichment, of unmoderated and unreflected plutonium metal, or of homogeneous uranium solutions. The simplicity of the method lies in the fact that the two input constants required can be obtained from two delayed-critical experiments in simple geometry provided that the neutron energy spectrum is the same in all cases, or from two subcritical assemblies if the multiplication factors have been accurately determined and the neutron energy spectrum is the same as that in a critical assembly.

Acknowledgment

The author wishes to acknowledge the assistance of J. Knight and E. Whitesides of the Central Data Processing Facility at Oak Ridge in performing the transport theory calculations and to G. W. Morrison, also of the CDPF, in carrying out the required programming for the Monte Carlo calculations. The advice of D. Irving of Oak Ridge National Laboratory in explaining the O5R Code was invaluable.

References

1. G. E. Hansen, "Physics of Fast and Intermediate Reactors," Proc. of a Seminar, Vol. 1, p. 453 IAEA Austria (1962).
2. John T. Mihalczo, Nucl. Sci. Eng. 20, 60 (1964).
3. John T. Mihalczo, Trans. Amer. Nucl. Soc. 6, 60 (1963).
4. John T. Mihalczo, Neutron Phys. Div. Ann. Progr. Rept. for Period Ending Aug. 1, 1963, ORNL-3499, Vol. I, 64 (1963).
5. J. T. Thomas, Critical Three-Dimensional Arrays of Neutron-Interacting Units, Part II. U(93.2 Metal, ORNL TM-868 (July 1964); J. T. Thomas, Trans. Amer. Nucl. Soc. 6, 169 (1963).
6. J. T. Mihalczo and D. C. Irving, Trans. Amer. Nucl. Soc. 7, 287 (1964).
7. J. T. Mihalczo, Trans. Amer. Nucl. Soc. 8, 201 (1965).
8. W. J. Worlton and B. G. Carlson, private communication.
9. B. G. Carlson and G. I. Bell, Proc. Intern. Conf. Peaceful Uses of Atomic Energy, 2nd Geneva, 1958, 16, 535 (1959).
10. D. C. Irving, R. M. Freestone, Jr., and F. B. K. Kam, O5R, A General Purpose Monte Carlo Neutron Transport Code, ORNL-3622 (February 1965).

APPENDIX A

Table A.1. Results of Exact Solutions of the One-Velocity Transport Equation with Isotropic Scattering for Uniform Spheres Without Reflectors^a

$\nu\Sigma_f/\Sigma_t$	Radius (Mean Free Paths, Σ_t^{-1})
0.02	12.027
0.05	7.2772
0.1	4.8727
0.2	3.1720
0.4	1.9854
0.6	1.4761
0.8	1.1833
1.0	0.9906

a. From Ref. 9.

APPENDIX B

Comparison of Effects of Assumed Neutron Source Distribution
on the Results of Calculation for a Uranium Sphere

The effects of the assumed initial source distribution on the multiplication factor, some of the production probabilities F_{ij} , average number of collisions before loss, mean time to fission, and mean time to loss, are given in Table B.1 for a point, uniform or cosine initial source distribution. To within the standard deviations these quantities do not depend on the choice of the initial source distribution. Table B.2 gives the results of the matrix iteration on the initial source distribution. In each of the three cases of the table, the matrix of the production probabilities is obtained from the results of the O5R calculation for the particular source considered. After eight to ten iterations the source distribution converged to five decimal places. In these calculations the sphere was divided into five concentric regions of equal volume.

Table B.1. Comparison of the Effect of Various Initial Neutron Source Distributions on Calculated Results for Uranium Sphere (Godiva I)^a

	Point Source ^b	Uniform Source ^c	Cosine Source ^d
05R k_{eff}	1.003 ± 0.011^e	1.005 ± 0.009	1.015 ± 0.011
Matrix k_{eff}	1.013	0.995	1.015
Production Probabilities			
F_{11}	0.607 ± 0.014	0.616 ± 0.012	0.598 ± 0.11
F_{22}	0.361 ± 0.007	0.323 ± 0.007	0.349 ± 0.009
F_{33}	0.248 ± 0.008	0.249 ± 0.009	0.255 ± 0.007
F_{44}	0.183 ± 0.009	0.193 ± 0.009	0.185 ± 0.009
F_{55}	0.128 ± 0.009	0.143 ± 0.006	0.138 ± 0.009
Average number of collisions before loss	2.56	2.48	2.54
Mean time ^f to loss (sec)	11.0 ± 0.07	10.97 ± 0.07	11.07 ± 0.08
Mean time ^f to fission (sec)	9.3 ± 0.09	9.2 ± 0.11	9.3 ± 0.13

a. 30 batches, 400 source neutrons per batch.

b. Point source at center, k_{eff} of batch 1 = 1.38.

c. k_{eff} of batch 1 = 0.77.

d. Zero of cosine at $r = 8.81$ cm, k_{eff} of batch 1 = 1.09.

e. All errors are standard deviations.

f. Neutron velocity assumed in the calculation is 1 cm/sec.

Table B.2. Matrix Iteration^a on Point, Uniform and Cosine Initial Neutron Source Distribution in Godiva

Iteration on Source Distribution	Region 1	Region 2	Region 3	Region 4	Region 5
Source Distribution for Point Source at Center					
1	1.0				
2	0.47387	0.21318	0.13958	0.10041	0.07296
3	0.36501	0.23887	0.17412	0.12977	0.09223
4	0.33665	0.24333	0.18339	0.13853	0.09810
5	0.32876	0.24428	0.18597	0.14111	0.09987
6	0.32652	0.24452	0.18671	0.14186	0.10039
7	0.32588	0.24458	0.18692	0.14208	0.10054
8	0.32570	0.24460	0.18698	0.14214	0.10058
9	0.32564	0.24460	0.18700	0.14216	0.10060
10	0.32563	0.24461	0.18700	0.14216	0.10060
30	0.32562	0.24461	0.18700	0.14216	0.10060
Source Distribution for Uniform Source					
1 ^b	0.1900	0.17500	0.22500	0.20250	0.20750
2	0.28474	0.22600	0.19808	0.16593	0.12524
3	0.31940	0.23373	0.18914	0.14863	0.10910
4	0.33032	0.23492	0.18609	0.14358	0.10509
5	0.33361	0.23512	0.18512	0.14214	0.10400
6	0.33459	0.23516	0.18482	0.14173	0.1037
7	0.33488	0.23517	0.18474	0.14161	0.10361
8	0.33496	0.23517	0.18471	0.14157	0.10358
9	0.33499	0.23517	0.18470	0.14156	0.10357
30	0.33500	0.23517	0.18470	0.14156	0.10357
Source Distribution for Cosine Source with Zero at $x = y = z = 8.81$ cm					
1 ^c	0.35750	0.28750	0.16250	0.1075	0.0850
2	0.33711	0.25299	0.18573	0.12896	0.09520
3	0.32967	0.24928	0.18899	0.13348	0.09857
4	0.32742	0.24884	0.18977	0.13453	0.09944
5	0.32677	0.24878	0.18998	0.13480	0.09967
6	0.32659	0.24977	0.19004	0.13487	0.09973
7	0.32654	0.24877	0.19006	0.13489	0.09975
8	0.32652	0.24877	0.19007	0.13489	0.099751
30	0.32652	0.24877	0.19007	0.13490	0.09975

a. Convergence criteria $\sqrt{\sum(S_M - S_C)^2} < \text{prescribed number}$.

b. Statistical sampling of 400 neutrons from uniform source.

c. Statistical sampling from 400 neutrons from cosine source.

APPENDIX C

Description and Relative Location of Nine Variously Shaped
Metal Units Constituting a Critical Array

The uranium-metal units arranged in a circle surrounding a central one, shown in Fig. 5, are described in the following order: first the center unit, then the upper unit of the ring of eight, followed by the others taken clockwise around the circle. The origin of the coordinate system selected to describe the array was located on the axis of the lower cylindrical piece of the center unit, 1.755 cm above the lower surface. The coordinates of the center of the lower surface of each of the units on the circle locate these units. The nearly vertical axis of each outer unit is tilted toward the truly vertical axis of the system.

The central unit consisted of a 11.514-cm-diam cylinder, 2.690 cm high, on which a parallelepiped, 12.700 x 12.700 x 5.718 cm high, was located so that vertical planes, designated A and B, defined by two adjacent sides of the parallelepiped were tangent to the lateral surface of the cylinder. A 12.164-cm-diam hemisphere was placed on top of the parallelepiped so that two vertical planes, also defined by adjacent sides of the parallelepiped, were tangent to the hemisphere. (One of these two planes is A; the other is parallel to B and on the opposite side of the parallelepiped.) [Side and top views of this unit and its position relative to two other units of this arrangement are shown in Fig. C-1.] The masses of the hemisphere, parallelepiped and cylinder comprising the central unit were 8.840, 17.200, and 5.247 kg, respectively. The overall density was 18.713 g/cm³. The coordinates of a point in the center of the

base of this central unit are $x = 0$, $y = 0$, and $z = -1.755$ cm.

The unit at the top of Fig. 5 was a parallelepiped with a 12.703×12.703 cm base containing 38.497 kg with a density of 18.625 g/cm^3 . The height of this unit varied in three steps as shown in Fig. C-1 and two of its sides are in the same plane as two sides of the parallelepiped of the central unit. The top of this parallelepiped is tilted 1.35 deg toward the axis of the system. The coordinates of a point in the center of the base of this unit were $x = -15.66$, $y = -6.53$, and $z = +0.15$ cm.

The descriptions of the next three cylinders in the ring are given in Table C-1.

The unit at the bottom of the ring consisted of a parallelepiped with a base 12.703×7.620 cm and a height of 8.910 cm. The center of this parallelepiped lies in the same vertical plane as do the centers of the parallelepipeds in the central unit and in the unit at the top of Fig. 5. A 9.146 -cm-diam cylinder 4.320 cm high was located on top of this parallelepiped so that the plane bisecting the parallelepiped also bisected the cylinder. A plane coincident with the inner 7.620×8.910 cm face of the parallelepiped was tangent to the surface of the cylinder. A side and top view of this unit is also given in Fig. C-1. The total mass of this unit was 21.386 kg, 5.286 kg being in the cylinder, and the density was 18.689 g/cm^3 . Its top was tilted 2.58 deg toward the axis of the system. The coordinates of the center of the base of the parallelepiped were $x = 17.889$, $y = 2.03$, and $z = 0.29$ cm. A sketch of this unit is given in Fig. C-1.

The description of the next three cylinders in the ring is given in Table C-1.

Table C-1. Description of Six Cylindrical Units in the Eight-Unit Ring

Unit Number ^a	Mass (kg of U)	Uranium Density (g/cm ³)	Diameter (cm)	Height (cm)	Coordinate of Point in Center of Base (cm)			Rota- tional ^a Angle
					x	y	z	
2	15.768	18.733	9.111	12.918	-10.177	10.411	0.111	1.40
3	26.216	18.748	11.522	13.475	0	15.762	0.174	1.173
4	15.720	18.734	9.105	12.969	10.245	10.585	0.156	1.97
6	15.727	18.717	9.109	12.974	13.173	- 8.194	0.134	1.68
7	26.160	18.766	11.499	13.475	4.954	-16.357	0.140	1.40
8	15.755	18.763	9.113	12.954	- 6.338	-14.091	0.087	1.10

- a. The units are numbered clockwise beginning with the parallelepiped uppermost in the ring.
- b. Angle between axis of unit and the vertical.

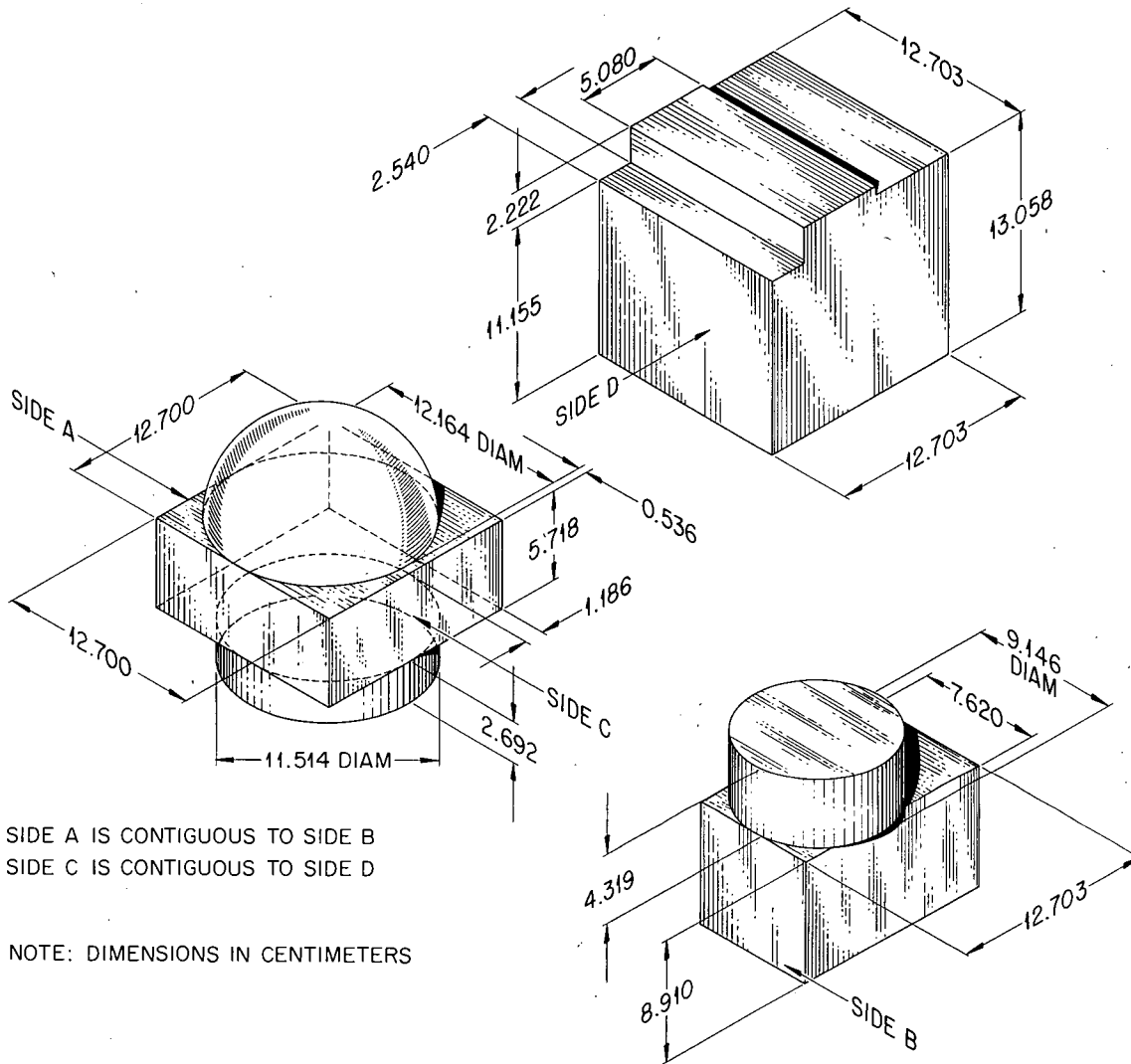


Fig. C-1. Three Units Used in Array Pictured in Fig. 5.

INTERNAL DISTRIBUTION

- | | | | |
|--------|-------------------|--------|-------------------------------|
| 1- 5. | L. S. Abbott | 46-50. | G. W. Morrison, ORCDFP |
| 6-10. | A. D. Callihan | 51. | R. W. Peelle |
| 11. | N. Betz | 52. | A. M. Perry |
| 12. | V. R. Cain | 53. | E. G. Silver |
| 13. | R. S. Carlsmith | 54. | J. G. Sullivan |
| 14. | H. C. Claiborne | 55. | J. T. Thomas |
| 15. | F. H. S. Clark | 56. | M. L. Tobias |
| 16. | E. L. Compere | 57. | D. K. Trubey |
| 17. | R. R. Coveyou | 58. | D. R. Vondy |
| 18. | I. B. Fowler | 59. | J. W. Wachter |
| 19. | N. M. Greene | 60. | J. W. Webster |
| 20. | R. Gwin | 61. | G. E. Whitesides, ORCDFP |
| 21. | D. C. Hamilton | 62. | K. J. Yost |
| 22. | L. B. Holland | 63-65. | Central Research Library |
| 23-26. | D. C. Irving | 66. | Document Reference Section |
| 27. | L. Jung | 67-70. | Laboratory Records Department |
| 28. | F. B. K. Kam | 71. | Laboratory Records-ORNL-RC |
| 29. | W. E. Kinney | 72. | ORNL Patent Office |
| 30. | R. E. Maerker | 73. | G. Dessauer (Consultant) |
| 31. | F. C. Maienschein | 74. | M. L. Goldberger (Consultant) |
| 32-40. | B. F. Maskewitz | 75. | M. V. Spencer (Consultant) |
| 41-45. | J. T. Mihalcz | 76. | M. H. Kalos (Consultant) |

EXTERNAL DISTRIBUTION

- 77-91. Division of Technical Extension (DTIE)
- 92. Research and Development Division (ORO)
- 93. C. R. Richey, GE Company, HAPO, Richland, Washington
- 94. H. C. Paxton, Los Alamos Scientific Laboratory
- 95. N. Provost, Lawrence Radiation Laboratory, Livermore
- 96. C. B. Mills, Los Alamos Scientific Laboratory
- 97. C. L. Schuske, Rocky Flats Plant, Dow Chemical Company
- 98. A. E. Profio, General Atomic, San Diego, California
- 99. N. C. Francis, Knolls Atomic Power Laboratory, Schenectady, New York
- 100. J. R. Beyster, General Atomic, San Diego, California
- 101. S. Strauch, U. S. Atomic Energy Commission, Washington, D. C.